Calculation of photoemission spectra of the doped Mott insulator $La_{1-x}Sr_xTiO_3$ using LDA+DMFT(QMC)

I.A. Nekrasov[1,a], K. Held[2,b], N. Blümer[2], A.I. Poteryaev[1], V.I. Anisimov[1], and D. Vollhardt[2]

[1] Institute of Metal Physics, Russian Academy of Sciences-Ural Division, 620219 Yekaterinburg GSP-170, Russia
[2] Theoretische Physik III, Elektronische Korrelationen und Magnetismus, Universität Augsburg, 86135 Augsburg, Germany

Abstract. The spectral properties of $La_{1-x}Sr_xTiO_3$, a doped Mott insulator with strong Coulomb correlations, are calculated with the *ab initio* computational scheme LDA+DMFT(QMC). It starts from the non-interacting electronic band structure as calculated by the local density approximation (LDA), and introduces the missing correlations by the dynamical mean-field theory (DMFT), using numerically exact quantum Monte-Carlo (QMC) techniques to solve the resulting self-consistent multi-band single-impurity problem. The results of the LDA+DMFT(QMC) approach for the photoemission spectra of $La_{1-x}Sr_xTiO_3$ are in good agreement with experiment and represent a considerable qualitative and quantitative improvement on standard LDA calculations.

PACS. 71.27.+a Strongly correlated electron systems; heavy fermions – 74.25.Jb Electronic structure – 79.60.-i Photoemission and photoelectron spectra

1 Introduction

At present, the electronic properties of solids are investigated by two essentially separate communities, one using model Hamiltonians in conjunction with many-body techniques, the other employing density functional theory (DFT) [1]. DFT and its local density approximation (LDA) have the advantage of being *ab initio* approaches which do not require empirical parameters as input. Indeed, they are highly successful techniques for the calculation of the electronic structure of real materials [2]. However, in practice DFT/LDA is seriously restricted in its ability to describe strongly correlated materials where the on-site Coulomb interaction is comparable with the band width. Here, the model Hamiltonian approach is more general and powerful since there exist systematic theoretical techniques to investigate the many-electron problem with increasing accuracy. Nevertheless, the uncertainty in the choice of the model parameters and the technical complexity of the correlation problem itself prevent the model Hamiltonian approach from being a flexible or reliable enough tool for studying real materials. The two approaches are therefore complementary. In view of the individual power of DFT/LDA and the model Hamiltonian approach, respectively, it would be highly desirable to be able to combine these techniques, thereby creating an enormous potential for future *ab initio* investigations of all real materials, including, *e.g.*, f-electron systems and Mott insulators. One of the first successful attempts in this direction was the LDA+U method [3], which combines LDA with a basically static, *i.e.*, Hartree-Fock-like, mean-field approximation for a multi-band Anderson lattice model (with interacting and non-interacting orbitals). This method proved to be a very useful tool in the study of long-range ordered, insulating states of transition metals and rare-earth compounds. However, the paramagnetic metallic phase of correlated electron systems such as high-temperature superconductors and heavy-fermion systems clearly requires a treatment that goes beyond a static mean-field approximation and includes dynamical effects, *e.g.*, the frequency dependence of the self-energy.

During the last decade a new many-body approach was developed which is especially well-suited for the investigation of strongly correlated metals – the dynamical mean-field theory (DMFT) [4–6]. It becomes exact in the limit of high lattice coordination numbers [7] and preserves the dynamics of local interactions; hence it represents a *dynamic* mean-field approximation. In this non-perturbative approach, the lattice problem is mapped onto an effective Anderson impurity model with a hybridization function which has to be determined self-consistently. To solve the effective impurity problem one can either use approximative techniques such as iterated perturbation theory (IPT) [8,6] and the non-crossing approximation (NCA) [9–11], or employ numerical techniques like quantum Monte-Carlo simulations (QMC) [12], exact diagonalization (ED) [13,6], and numerical renormalization group (NRG) [14]. In principle, QMC, ED and NRG are exact

[a] e-mail: nekrasov@ifmlrs.uran.ru
[b] e-mail: held@physik.uni-augsburg.de

methods, but require an extrapolation: discretization of the imaginary time $\Delta\tau \to 0$ (QMC), the number of lattice sites of the respective impurity model $n_s \to \infty$ (ED), and the parameter for logarithmic discretization of the conducting band $\Lambda \to 1$ (NRG), respectively.

In principle, the main idea of the LDA+U method [3] (*i.e.*, complementing the LDA band structure by a screened Coulomb interaction between localized tight-binding orbitals) can be practically applied with more refined approximation schemes [15–20]. Indeed, a calculation scheme supplementing LDA with DMFT to include dynamic effects was first formulated by Anisimov *et al.* [15] and was used to calculate the photoemission spectra of $La_{1-x}Sr_xTiO_3$, a doped Mott-insulator and strongly correlated paramagnetic metal, in connection with IPT [15] and NCA [20]. The LDA++ approach by Lichtenstein and Katsnelson [16] formulates a very similar strategy and was recently applied to investigate correlation effects in iron [21,22]. Both IPT and NCA are approximative methods to solve the effective single-impurity problem in the LDA+DMFT scheme. They have the advantage of being numerically inexpensive, but their reliability, especially in the case of multi-band systems with particle densities off half-filling, is in principle uncertain. In this situation, it is clearly desirable to employ a controlled computation scheme to obtain numerically exact results from LDA+DMFT. The QMC method is such a scheme and was already applied by Lichtenstein and collaborators to calculate the magnetic excitation spectrum of ferromagnetic iron [22] and the photoemission spectra of Sr_2RuO_4 [23]. In the present paper we report on our implementation of the LDA+DMFT(QMC) technique and the results obtained with it for the photoemission spectra of $La_{1-x}Sr_xTiO_3$.

2 Computational scheme

2.1 Local density approximation (LDA)

The main problem in combining LDA and model Hamiltonian approaches comes from the fact that their foundations are very different. The LDA employs a functional of the electron density, while Hubbard and Anderson models are formulated in terms of localized, site-centered, atomic-like orbitals. In order to merge the approaches it is necessary to write LDA equations in the basis of such orbitals. There is one variant of the LDA method, based on tight-binding linearized muffin-tin orbitals in the orthogonal approximation (TBLMTO) [24], which is naturally realized in such a basis. The corresponding Hamiltonian can be written as

$$H_{\mathrm{LDA}} = \sum_{ilm,jl'm',\sigma} (\delta_{ilm,jl'm'}\varepsilon_{ilm}\hat{n}^{\sigma}_{ilm} + t_{ilm,jl'm'}\hat{c}^{\sigma\dagger}_{ilm}\hat{c}^{\sigma}_{jl'm'}), \qquad (1)$$

where i, j are site indices, l, m, l', m' are orbital indices, σ is a spin index, and operators carry a hat.

Taking this expression as the non-interacting part of a multi-band periodic Anderson model, one may complement it by a correlation term describing the local contributions to the Coulomb interaction

$$H_{\mathrm{corr}} = \frac{1}{2}{\sum_{il,m\sigma m'\sigma'}}' U^{il}_{mm'}\,\hat{n}_{ilm\sigma}\hat{n}_{ilm'\sigma'}. \qquad (2)$$

The prime on the sum indicates that at least two of the indices on different operators have to be different. Here, $U^{il}_{mm'}$ denotes the direct Coulomb integral. The much smaller exchange integral and other local contributions of the Coulomb interaction have been neglected. Furthermore, non-local Coulomb contributions are not considered in H_{corr}. Note, that the largest non-local contributions is the nearest-neighbor density-density interaction which, to leading order in Z (Z: number of nearest-neighbor sites), yields only the Hartree term [25] which is already taken into account in the LDA. In an actual calculation, it is not possible to include the local two-particle interaction terms between all orbitals appearing in (2) since the number of states grows exponentially with increasing orbital quantum number. Thus, one usually concentrates on a certain subset of correlations and treats the influence of the remaining states *via* the use of effective, screened interaction parameters for the shells under consideration. In this spirit, we will assume in the following that it is only necessary to take the Coulomb interaction for the d-shell of the transition metal ions ($i = i_d$ and $l = l_d$) explicitly into account; therefore the indices il will be omitted. The correlation part of the Hamiltonian then acts only on the d-wave functions of the transition metal ions. All other valence orbitals will be treated as bands of itinerant electrons which are well described by the LDA.

One must take into account, however, that the Coulomb interaction is already present in LDA in some averaged way. Hence, to avoid double-counting one needs to subtract this term from the LDA-Hamiltonian. Unfortunately, there exists no direct microscopic or diagrammatic link between the Hubbard model approach and LDA, and it is thus not possible to express the LDA energy rigorously *via* the $d-d$ Coulomb interaction parameter U (except for the atomic limit where one can make a connection between the Coulomb parameter U of the Hubbard model and the second derivative of the atomic total energy as a function of the number of electrons). While it is known that LDA eigenvalues are rather bad approximations for excitation energies of systems with strong Coulomb interactions, the LDA *total* energy as a function of the number of electrons is a much better approximation for the exact functional. Furthermore, the values of U obtained from LDA calculations often agree well with experimental data and more rigorous calculations.

Therefore one may expect that the LDA part of the Coulomb interaction energy is well approximated by the averaged value of the Coulomb interaction energy in (2)

$$E_{\mathrm{corr}} := \frac{1}{2}Un_d(n_d - 1). \qquad (3)$$

Here, U is the mean value of the Coulomb interaction and may be obtained from a first-principles constrained

LDA calculation [26] or from experiment, *e.g.* high-energy spectroscopy; n_d is the total number of d-electrons.

In LDA, one-electron energies are defined as derivatives of the total energy as a function of the occupation numbers for the corresponding states. Hence, the one-electron energy level for the *non-interacting* d-states is obtained by [15]

$$\varepsilon_d^0 := \frac{\mathrm{d}}{\mathrm{d}n_d}(E_{\mathrm{LDA}} - E_{\mathrm{corr}}) = \varepsilon_d^{\mathrm{LDA}} - U(n_d - \frac{1}{2}) \qquad (4)$$

with $\varepsilon_d^{\mathrm{LDA}} := \frac{\mathrm{d}}{\mathrm{d}n_d} E_{\mathrm{LDA}}$, and E_{LDA} being the total energy calculated from H_{LDA}.

Then, the new non-interacting Hamiltonian will have the form

$$H^0_{\mathrm{LDA}} = \sum_{ilm,jl'm',\sigma} (\delta_{ilm,jl'm'}\varepsilon^0_{ilm}\hat{n}^\sigma_{ilm} + t_{ilm,jl'm'}\hat{c}^{\sigma\dagger}_{ilm}\hat{c}^\sigma_{jl'm'}),$$

where $\varepsilon^0_{ilm} := \varepsilon_{ilm}\,(1-\delta_{l,l_d}) + \varepsilon^0_d\delta_{l,l_d}$. In reciprocal space, the matrix elements of the operator H^0_{LDA} are given by:

$$(H^0_{\mathrm{LDA}}(\mathbf{k}))_{qlm,q'l'm'} = (H_{\mathrm{LDA}}(\mathbf{k}))_{qlm,q'l'm'} - \delta_{qlm,q'l'm'}\delta_{ql,q_dl_d}U(n_d - \frac{1}{2}). \quad (5)$$

Here q is an index of the atom in the elementary unit cell, $(H_{\mathrm{LDA}}(\mathbf{k}))_{qlm,q'l'm'}$ is the matrix element in k-space of H_{LDA}, and q_d denotes the d-atoms in the unit cell. This non-interacting part H^0_{LDA}, taken together with the interaction part (2),

$$H = H^0_{\mathrm{LDA}} + H_{\mathrm{corr}} \qquad (6)$$

forms the *ab initio* Hamiltonian H for a particular material under investigation.

2.2 Dynamical mean-field theory (DMFT)

In general, the investigation of the correlated-electron Hamiltonian H is too complicated to allow for an exact solution or even a numerical investigation with more than about 10 sites. Here, the DMFT [4–6] is a powerful approximation scheme which takes into account electronic correlations and, in particular, correctly describes the formation of a coherent quasiparticle band and incoherent Hubbard bands.

The DMFT maps the lattice problem onto a single-site problem, which is equivalent to a multi-band single-impurity Anderson model, with the self-consistency condition [15] (the k-integrated Dyson equation)

$$G_{qlm,q'l'm'}(z) = \int \frac{\mathrm{d}\mathbf{k}}{V_{\mathrm{B}}} \; [z\delta_{qlm,q'l'm'} - (H^0_{\mathrm{LDA}}(\mathbf{k}))_{qlm,q'l'm'} - \delta_{ql,q_dl_d}\Sigma_{qlm,q'l'm'}(z)]^{-1}. \qquad (7)$$

Here, $[...]^{-1}$ implies the inversion of the matrix with elements $n\,(=qlm)$, $n'(=q'l'm')$, and integration extends over the Brillouin zone with volume V_{B}. In the present study we consider a cubic-crystal structure and assume only the t_{2g} orbitals to be interacting. Due to the high symmetry of the crystal, these three t_{2g} orbitals are degenerate. Without symmetry breaking, the Green function and the self-energy remain degenerate, *i.e.*, $G_{qlm,q'l'm'}(z) = G(z)\delta_{qlm,q'l'm'}$ and $\Sigma_{qlm,q'l'm'}(z) = \Sigma(z)\delta_{qlm,q'l'm'}$ for $l = l_d$ and $q = q_d$ (where l_d and q_d denote the Ti t_{2g} orbitals). If the partially filled band under consideration is well separated from other bands, as in the case of $La_{1-x}Sr_xTiO_3$ and other transition metal oxides, one can describe the physics of the partially filled band at the Fermi energy approximately by an effective three band Hamiltonian $H^{0\,\mathrm{eff}}_{\mathrm{LDA}}$, *e.g.*, by downfolding to a basis with t_{2g} orbitals only. One obtains (indices $l = l_d$ and $q = q_d$ suppressed):

$$G_{mm'}(z) = \int \frac{\mathrm{d}\mathbf{k}}{V_{\mathrm{B}}}[(z-\Sigma(z))\delta_{m,m'} - (H^{0\,\mathrm{eff}}_{\mathrm{LDA}}(\mathbf{k}))_{m,m'}]^{-1}. \quad (8)$$

Due to the diagonal structure of the self-energy the interacting Green function can be expressed *via* the non-interacting Green function $G^0(z)$:

$$G(z) = G^0(z - \Sigma(z)) = \int \mathrm{d}\omega \frac{\rho^0(\omega)}{z - \Sigma(z) - \omega}, \qquad (9)$$

Thus, it is possible to use the Hilbert transformation of the unperturbed LDA-calculated density of states $\rho^0(\omega)$ and we do so in the following. This approximation is justified if the hybridization between the t_{2g} orbitals and the other orbitals is rather weak as in the case of $LaTiO_3$.

The DMFT single-site problem depends on $\mathcal{G}^{-1} = G^{-1} + \Sigma$ and can be formulated in terms of Grassmann variables ψ and ψ^*. For the local Green function at a Matsubara frequency $\omega_\nu = (2\nu+1)\pi/\beta$, orbital index m, and spin σ one obtains:

$$G^\sigma_{\nu m} = -\frac{1}{\mathcal{Z}}\int \mathcal{D}[\psi]\mathcal{D}[\psi^*]\psi^\sigma_{\nu m}\psi^{\sigma *}_{\nu m}\mathrm{e}^{\mathcal{A}[\psi,\psi^*,\mathcal{G}^{-1}]}, \qquad (10)$$

where the single-site action $\mathcal{A}$ is given by

$$\mathcal{A}[\psi,\psi^*,\mathcal{G}^{-1}] = \sum_{\nu,\sigma,m}\psi^{\sigma *}_{\nu m}(\mathcal{G}^\sigma_{\nu m})^{-1}\psi^\sigma_{\nu m} - \frac{U}{2}\sum_{(m\sigma)\neq(m\sigma')}\int_0^\beta \mathrm{d}\tau\,\psi^{\sigma *}_m(\tau)\psi^\sigma_m(\tau)\psi^{\sigma' *}_{m'}(\tau)\psi^{\sigma'}_{m'}(\tau). \quad (11)$$

2.3 Quantum Monte-Carlo method (QMC)

To solve the effective single-site problem defined above we will apply the QMC method which allows for a numerically exact solution [12]. To this end, the imaginary time is first discretized into Λ steps of size $\Delta\tau$ ($\Delta\tau = 0.25\,\mathrm{eV}^{-1}$ throughout this work), and $\tau_t := t\Delta\tau$ with integer t.

Then, in a second step, the Hubbard-Stratonovich transformation

$$\exp \quad \frac{\Delta\tau U}{2}(\psi^{\sigma *}_{mt}\psi^{\sigma}_{mt} - \psi^{\sigma' *}_{m't}\psi^{\sigma'}_{m't})^2 \quad = \\ \frac{1}{2}\sum_{s^t_{m\sigma;m'\sigma'}=\pm 1} \exp\left\{\lambda s^t_{m\sigma;m'\sigma'}(\psi^{\sigma *}_{mt}\psi^{\sigma}_{mt} - \psi^{\sigma' *}_{m't}\psi^{\sigma'}_{m't})\right\} \quad (12)$$

is employed, which replaces the interacting system by a sum of $2^{(2M^2-M)\Lambda}$ different non-interacting systems, where M is the number of interacting orbitals. Each non-interacting system can be solved by a Gauss integration which yields a contribution $(\mathbf{M^s})^{-1}\det(\mathbf{M^s})$ to the Green function in imaginary time, parameterized by (t, t'), where

$$[\mathbf{M}^{\sigma\mathbf{s}}_m]_{tt'} = \Delta\tau^2 \ \ (\mathbf{G}^{\sigma}_m)^{-1} + \Sigma^{\sigma}_{m\ tt'} \\ -\delta_{tt'}\sum_{m'\sigma'} \lambda_{m\sigma;m'\sigma'}\ \tilde{\sigma}_{m\sigma;m'\sigma'}\ s^t_{m\sigma;m'\sigma'}. \quad (13)$$

Here, $\tilde{\sigma}_{m\sigma;m'\sigma'} = 2\Theta(\sigma' - \sigma + \delta_{\sigma\sigma'}[m' - m]) - 1$ has a different sign if $(m\sigma)$ and $(m'\sigma')$ are exchanged. Since a full summation over all non-interacting systems is computationally impossible, the Monte-Carlo method is employed for importance sampling. Details of the one-band QMC algorithm in the context of DMFT can be found in references [6,12] and for the band-degenerate case in reference [27].

3 Results and discussion

The stoichiometric compound $LaTiO_3$ has a perovskite crystal structure with a small orthorhombic distortion ($\angle$ Ti − O − Ti $\approx$ 155°) [28]. Below $T_N = 125$ K [29] it is an antiferromagnetic insulator [30] with a Ti magnetic moment of 0.45 μ_B and a small energy gap of approximately 0.2 eV [31,32]. At doping $x = 0.05$, $La_{1-x}Sr_xTiO_3$ undergoes an insulator-to-metal transition and becomes a correlated paramagnetic metal with a strongly enhanced susceptibility and electronic specific heat coefficient [33].

The standard LDA calculation for undoped $LaTiO_3$ yields a density of states (Fig. 1) which is typical for early transition metal oxides with a completely filled $2p$ oxygen band ranging from −8.2 eV to −4.0 eV and a partially filled Ti-$3d$ band above it. Since the Ti-ion has an octahedral coordination of oxygen ions, the Ti-$3d$ band is split into three degenerate t_{2g} and two degenerate e_g subbands which do not mix. Titanium is three-valent in $LaTiO_3$ and the corresponding formal ionic configuration is d^1. This implies a partially filled t_{2g} subband containing one electron with a total capacity of six electrons. The e_g subband is empty and situated just above the t_{2g} subband. In order to simplify our calculations the real orthorhombic crystal structure was replaced by a cubic structure with the same volume. This approximation leads to a slight overestimation of the effective bandwidth.

The t_{2g} band is the only partially filled band and is well separated from other bands. Therefore in our DMFT

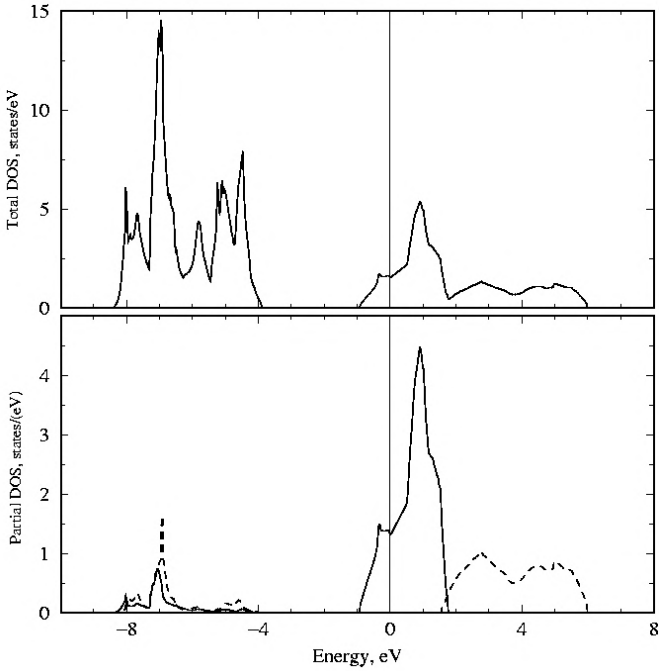

Fig. 1. Densities of states of $LaTiO_3$ calculated with LDA-LMTO. Upper figure: total density of states; lower figure: partial t_{2g} (solid lines) and e_g (dashed lines) densities of states.

calculation we took only Coulomb interactions between electrons in t_{2g} orbitals into account. The resulting problem is equivalent to a Hubbard model with three degenerate bands. The DMFT chemical potential was adjusted to yield the doping $x = 0.06$, *i.e.*, 0.94 electrons in the t_{2g} band. We employ equation (3) within constrained LDA [26], *i.e.*, changing the number of t_{2g}-electrons only, to calculate U. Our LMTO-ASA calculation (TB-LMTO-ASA code of Andersen and coworkers [24] version 47) yields a fully-screened Coulomb interaction of $U = 4.2$ eV within the basis Ti($4s$, $4p$, $3d$) La($6s$, $6p$, $5d$) O($2s$, $2p$) at a Wigner Seitz radius of 2.37 a.u. for Ti. Our result has to be compared to that of Solovyev *et al.* [34] who obtained $U = 3.2$ eV employing the ASA-LMTO method within orthogonal representation. This shows that the *ab initio* calculation of U, which is the interaction between particular (t_{2g}) orbitals, is rather sensitive to the orthogonality of the wave functions and, also, to the choice of the orbitals. Unless specified otherwise, we will, thus, use $U = 4$ eV and keep in mind that the inherent uncertainty is about 0.5 eV.

In Figure 2, the spectral function obtained from our LDA+DMFT(QMC) calculation at temperature $T \approx 1000$ K is compared with the non-interacting t_{2g} density of states. One can see the typical features of the spectra of strongly correlated systems: a lower Hubbard band, a well pronounced quasi-particle peak, and an upper Hubbard band. While for the non-interacting case 100% of the spectral weight is located in the quasi-particle band, the LDA+DMFT spectra are characterized by a spectral weight transfer from the quasiparticle band to the Hubbard bands and a narrowing of the quasiparticle band.

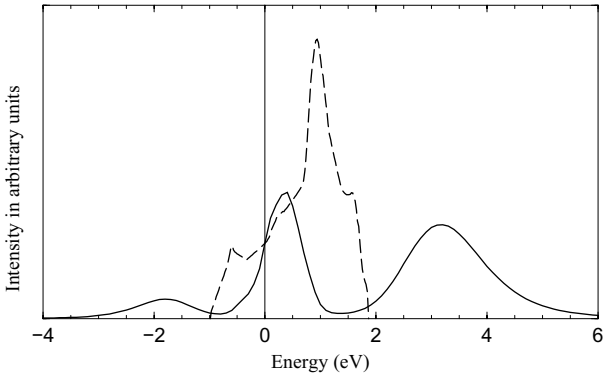

Fig. 2. Partial t_{2g} densities of states of $LaTiO_3$ calculated with LDA+DMFT(QMC) (solid lines) and LDA (dashed lines).

The QMC simulations performed in this paper to solve the effective multi-band single-impurity model provide a numerically exact solution, but require a large computational effort which restricted our calculations to temperatures of the order of $T = 0.1$ eV (≈ 1000 K). Since this technique yields results only at imaginary (Matsubara-) frequencies the calculation of the spectral function requires an analytic continuation of the spectral function *via*, *e.g.*, the maximum entropy method [35]. Previous LDA+DMFT investigations of the photoemission spectra of $La_{1-x}Sr_xTiO_3$ used a variant of IPT for doped multi-band systems [15] and NCA [20] to solve the DMFT-equations, *i.e.*, approximate techniques. In Figure 3, we compare the results obtained within these approximations with the numerically exact QMC simulation, all at $T \approx 1000$ K. One notes that within IPT the shape of the upper Hubbard band is not correct. Moreover, there is no quasiparticle peak at 1000 K, the reason being that IPT underestimates the Kondo temperature considerably such that the very narrow quasiparticle peak found at low temperatures (see right inset of Fig. 3) disappears already at about 250 K. A similarly narrow IPT quasiparticle peak was found in a three-band model study with Bethe-DOS by Kajueter and Kotliar [36]. While NCA comes off much better than IPT it still underestimates the width of the quasiparticle peak by a factor of two. Furthermore, the position of the quasiparticle peak is too close to the lower Hubbard band. In the left inset of Figure 3, the behavior at the Fermi level is shown. At the Fermi level, the NCA yields a spectral function which is almost by a factor two too small. The shortcomings of the NCA-results appear to result from the well-known problems which this approximation scheme encounters already in the single-impurity Anderson model at low temperatures and/or low frequencies [37,38]. Similarly, the deficiencies of the IPT-results are not entirely surprising in view of the semi-phenomenological nature of this approximation, especially for a system off half filling. This comparison shows that the choice of the method used to solve the DMFT equation is indeed important.

Photoemission spectroscopy of the early transition metal oxides provides a direct tool for the study of the electronic structure of strongly correlated materials. A

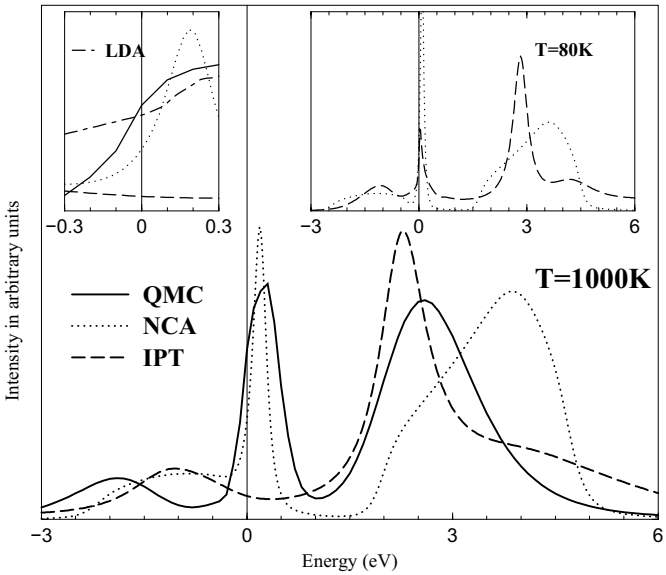

Fig. 3. Comparison of the spectral densities of $La_{1-x}Sr_xTiO_3$ ($x = 0.06$) as calculated by LDA+DMFT using the approximations IPT and NCA, with the numerically exact QMC-result at $T = 0.1$ eV, *i.e.*, approximately 1000 K, and $U = 4$ eV. Inset left: Behavior at the Fermi level including the LDA DOS. Inset right: NCA and IPT spectra for the temperature 80 K.

comparison of the experimental photoemission spectra [40] with results obtained from LDA and LDA+DMFT(QMC) at 1000 K [41] are shown in Figure 4. To take into account the uncertainty in U, we present results for $U = 3.2$, 4.25 and 5 eV. All spectra are multiplied with the Fermi step function and Gaussian-broadened with a broadening parameter of 0.3 eV to simulate the experimental resolution [40]. The LDA band structure calculation clearly fails to reproduce the broad band observed in the experiment at 1–2 eV below the Fermi energy [40]. Taking the correlations between the electrons into account, this lower band is easily identified as the lower Hubbard band whose spectral weight originates from the quasiparticle band at the Fermi energy and increases with U. The best agreement with experiment concerning the relative intensities of the Hubbard band and the quasi-particle peak and, also, the position of the Hubbard band is found for $U = 5$ eV [42,43]. The value $U = 5$ eV is still compatible with the *ab initio* calculation of this parameter. One should also note that the photoemission experiment is sensitive to surface properties. Due to the reduced coordination number at the surface, the bandwidth is likely to be smaller and the Coulomb interaction to be less screened, *i.e.*, larger. Both effects make the system more correlated and, thus, might also explain why better agreement is found for $U = 5$ eV. Besides, the polycrystalline nature of the sample also spin and orbital [44] fluctuation, not taken into account in the LDA+DMFT approach, could further reduce the quasiparticle weight.

In conclusion, the LDA+DMFT(QMC) approach is shown to be a workable computational scheme which merges the conventional band structure approach with

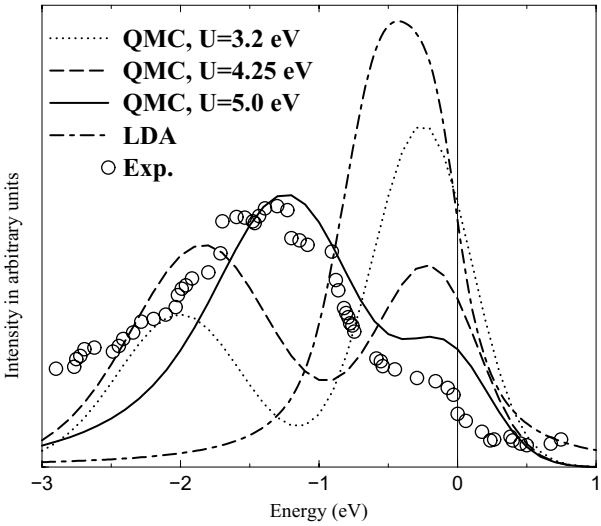

Fig. 4. Comparison of the experimental photoemission spectrum [40], the LDA result, and the LDA+DMFT(QMC) calculation for $LaTiO_3$ with 6% hole doping and different Coulomb interaction $U = 3.2$, 4.25, and 5 eV.

a recently developed many-body technique in combination with a numerically reliable evaluation method. Thereby, it provides a powerful tool for future *ab initio* investigations of real materials with strong electronic correlations. The LDA+DMFT(QMC) approach not only explains the existence of the lower Hubbard band in doped $LaTiO_3$, but also, in contrast to LDA, reproduces the qualitative picture of the spectral weight transfer from the quasiparticle band to the lower Hubbard band, the position of the lower Hubbard band, and the narrowing of the quasiparticle band.

We are grateful to R. Claessen, J. Lægsgaard, Th. Pruschke, G.A. Sawatzky, J. Schmalian, and M. Zölfl for useful discussions. This work was supported in part by the Sonderforschungsbereich 484 of the Deutsche Forschungsgemeinschaft and the Russian Foundation for Basic Research (RFFI-98-02-17275).

References

1. P. Hohenberg, W. Kohn, Phys. Rev. B **136**, 864 (1964); W. Kohn, L.J. Sham, Phys. Rev. **140**, 4A, A1133 (1965).
2. R.O. Jones, O. Gunnarsson, Rev. Mod. Phys. **61**, 689 (1989).
3. V.I. Anisimov, J. Zaanen, O.K. Andersen, Phys. Rev. B **44**, 943 (1991); V.I. Anisimov, F. Aryasetiawan, A.I. Lichtenstein, J. Phys. Cond. Matt. **9**, 767 (1997).
4. D. Vollhardt, in *Correlated Electron Systems*, edited by V.J. Emery (World Scientific, Singapore, 1993), p. 57.
5. Th. Pruschke, M. Jarrell, J.K. Freericks, Adv. in Phys. **44**, 187 (1995).
6. A. Georges, G. Kotliar, W. Krauth, M.J. Rozenberg, Rev. Mod. Phys. **68**, 13 (1996).
7. W. Metzner, D. Vollhardt, Phys. Rev. Lett. **62**, 324 (1989).
8. A. Georges, G. Kotliar, Phys. Rev. B **45**, 6479 (1992).
9. H. Keiter, J.C. Kimball, Phys. Rev. Lett. **25**, 672 (1970); N.E. Bickers, D.L. Cox, J.W. Wilkins, Phys. Rev. B **36**, 2036 (1987).
10. Th. Pruschke, N. Grewe, Z. Phys. B **74**, 439 (1989).
11. Th. Pruschke, D.L. Cox, M. Jarrell, Phys. Rev. B **47**, 3553 (1993).
12. J.E. Hirsch, R.M. Fye, Phys. Rev. Lett. **56**, 2521 (1986); M. Jarrell, Phys. Rev. Lett. **69**, 168 (1992); M. Rozenberg, X.Y. Zhang, G. Kotliar, Phys. Rev. Lett. **69**, 1236 (1992); A. Georges, W. Krauth, Phys. Rev. Lett. **69**, 1240 (1992).
13. M. Caffarel, W. Krauth, Phys. Rev. Lett. **72**, 1545 (1994).
14. R. Bulla, Adv. Sol. State Phys. (to be published), preprint `cond-mat/0003377`.
15. V.I. Anisimov, A.I. Poteryaev, M.A. Korotin, A.O. Anokhin, G. Kotliar, J. Phys. Cond. Matt. **9**, 7359 (1997).
16. A.I. Lichtenstein, M.I. Katsnelson, Phys. Rev. B **57**, 6884 (1998).
17. V. Drchal, V. Janiš, J. Kudrnovský, in *Electron Correlations and Material Properties*, edited by A. Gonis, N. Kioussis, M. Ciftan (Kluwer/Plenum, New York, 1999), p. 273.
18. J. Lægsgaard, A. Svane, Phys. Rev. B **58**, 12817 (1998).
19. Th. Wolenski, *Combining bandstructure and dynamical mean-field theory: A new perspective on V_2O_3*, Ph.D. thesis, Universität Hamburg 1998, Shaker Verlag, Aachen 1999.
20. M.B. Zölfl, Th. Pruschke, J. Keller, A.I. Poteryaev, I.A. Nekrasov, V.I. Anisimov, Phys. Rev. B **61**, 12810 (2000).
21. M.I. Katsnelson, A.I. Lichtenstein, J. Phys. Cond. Matt. **11**, 1037 (1999).
22. M.I. Katsnelson, A.I. Lichtenstein, Phys. Rev. B **61**, 8906 (2000)
23. A. Liebsch, A. Lichtenstein, Phys. Rev. Lett. **84**, 1591 (2000).
24. O.K. Andersen, Phys. Rev. B **12**, 3060 (1975); O. Gunnarsson, O. Jepsen, O.K. Andersen, Phys. Rev. B **27**, 7144 (1983).
25. E. Müller-Hartmann, Z. Phys. B **74**, 507 (1989); J. Wahle *et al.*, Phys. Rev. B **58**, 12749 (1998).
26. O. Gunnarson, O.K. Andersen, O. Jepsen, J. Zaanen, Phys. Rev. B **39**, 1708 (1989).
27. M.J. Rozenberg, Phys. Rev. B **55**, R4855 (1997); J.E. Han, M. Jarrell, D.L. Cox, Phys. Rev. B **58**, R4199 (1998); K. Held, D. Vollhardt, Eur. Phys. J. B **5**, 473 (1998).
28. D.A. MacLean, H.-N. Ng, J.E. Greedan, J. Solid State Chem. **30**, 35 (1979).
29. J.P. Gopel, J.E. Greedan, D.A. MacLean, J. Solid State Chem. **43**, 244 (1981).
30. M. Eitel, J.E. Greedan, J. Less-Common Met. **116**, 95 (1986).
31. Y. Okimoto, T. Katsufuji, Y. Okada, T. Arima, Y. Tokura, Phys. Rev. B **51**, 9581 (1995).
32. J.P. Goral, J.E. Greedan, D.A. MacLean, J. Solid State Chem. **43**, 244 (1982).
33. Y. Tokura, Y. Taguchi, Y. Okada, Y. Fujishima, T. Arima, K. Kumagai, Y. Iye, Phys. Rev. Lett. **70**, 2126 (1993).

34. I.V. Solovyev, N. Hamada, K. Terakura, Phys. Rev. B **53**, 7158 (1996).
35. For a review on the maximum entropy method see M. Jarrell, J.E. Gubernatis, Physics Reports **269**, 133 (1996). Here, the code of A. Sandvik was employed. Note, that the maximum entropy method is most reliable in the vicinity of the Fermi energy. At larger energies, the energy resolution becomes poorer.
36. H. Kajueter, G. Kotliar, Int. J. Mod. Phys. **11**, 729 (1997).
37. E. Müller-Hartmann, Z. Phys. B **57**, 281 (1984).
38. NCA is a self-consistent perturbation theory for the single-impurity Anderson model and is often a fast method to obtain results for this model and also within DMFT. However, NCA is known to violate Fermi liquid properties at temperatures much lower than the smallest energy scale of the problem and whenever charge excitations become important [37,39]. Hence, in some parameter ranges it fails to account for the proper low-energy physics and must therefore be applied with considerable care [39].
39. Th. Pruschke, D.L. Cox, M. Jarrell, Phys. Rev. B **47**, 3553 (1993).
40. A. Fujimori *et al.*, Phys. Rev. Lett. **69**, 1796 (1992). A. Fujimori *et al.*, Phys. Rev. B **46**, 9841 (1992). A qualitatively *and* quantitatively similar spectrum was obtained recently by Yoshida *et al.*, preprint `cond-mat/9911446`, with an experimental energy resolution of only 30 meV. One may suppose, however, that broadening effects due to the polycrystalline nature of the sample and surface effects are, then, larger than the instrumental resolution.
41. At present, QMC simulations of the DMFT equations are not feasible at the experimental temperature (80 K). We note, however, that no intrinsic temperature dependence was observed in the experiment [40], at least up to room temperature.
42. In Figure 4, the distance between the lower Hubbard band and the chemical potential is seen to decrease with increasing U. Note, however, that the upper Hubbard band is also shifted to higher energies.
43. If one multiplies the IPT and NCA results of Figure 3 with the Fermi function and employs a broadening of 0.3 eV one obtains a spectrum where the lower Hubbard band is nearer to the Fermi energy and which has a less pronounced minimum or shoulder between Hubbard and quasi-particle band.
44. B. Keimer *et al.*, preprint `cond-mat/0002014.`